World Journal of Advanced Research and Reviews
eISSN: 2581-9615 CODEN (USA): WJARAI
Cross Ref DOI: 10.30574/wjarr
Journal homepage: https://wjarr.com/

(RESEARCH ARTICLE)

Check for updates

Multimodality Imaging of Extra-Ovarian Lesions Simulating Ovarian Masses

AMAL AKAMMAR [1,*], HAJAR OUAZZANI CHAHDI [1], ISMAIL CHAOUCH [2], NIZAR EL BOUARDI [2], BADREEDDINE ALAMI [2], MOULAY YOUSSEF ALAOUI LAMRANI [2], MUSTAPHA MAAROUFI [2] and MERIEM BOUBBOU [1]

[1] *Department of Maternal and Child Radiology, Faculty of Medicine, Pharmacy and Dentistry of Fez, Sidi Mohamed Ben Abdellah University, Fez, MAR.*
[2] *Department of Radiology. Faculty of Medicine, Pharmacy and Dentistry of Fez, Sidi Mohamed Ben Abdellah University, Fez, MAR.*

World Journal of Advanced Research and Reviews, 2026, 30(03), 1060-1072

Publication history: Received on 08 May 2026; revised on 13 June 2026; accepted on 16 June 2026

Article DOI: https://doi.org/10.30574/wjarr.2026.30.3.1699

Abstract

Background: The female pelvis is a complex anatomical region where numerous extra-ovarian pathologies closely mimic ovarian masses. Misdiagnosis can lead to unnecessary surgery and delayed treatment. Accurate multimodality imaging interpretation is essential for appropriate patient management.

Objective: To describe the imaging characteristics, clinical context, and key differentiating features of the full spectrum of extra-ovarian pelvic pathologies identified in a retrospective single-center series, illustrating selected cases with representative imaging findings.

Methods: Retrospective study of 241 patients presenting with a pelvic mass on ultrasound (US), computed tomography (CT), and/or magnetic resonance imaging (MRI) at the Radiology Department of Hassan II University Hospital, Fez, Morocco, over a three-year period (January 2023–December 2025). Cases were classified based on histopathological and/or radiological findings.

Results: Twenty distinct extra-ovarian etiologies were identified across 241 cases, including tubal pathology (hydrosalpinx/hematosalpinx n=13, pyosalpinx/tubo-ovarian abscess n=23), adnexal ectopic pregnancy (n=13), adnexal torsion (n=27), peritoneal inclusion cyst (n=14), uterine vasculature (n=9), leiomyoma FIGO 7 (n=17), peritoneal carcinomatosis (n=12), peritoneal tuberculosis (n=8), appendicitis/diverticulitis (n=21), appendiceal mucocele (n=10), GIST (n=5), sigmoid tumor (n=7), necrotic lymphadenopathy (n=11), lymphoma (n=7), sarcoma (n=3), neurogenic tumors (n=4), pelvic pheochromocytoma (n=1), hematoma (n=23), and lymphocele (n=13). MRI was the definitive problem-solving modality in the majority of cases.

Conclusion: A systematic multimodality imaging approach combining anatomical compartment analysis, specific imaging signs, and clinical correlation enables accurate differentiation of extra-ovarian pelvic pathologies from true ovarian masses, preventing misdiagnosis and guiding optimal management. MRI remains the superior problem-solving tool in this context.

Keywords: Pelvic mass; Ovarian mimic; MRI; Extra-ovarian; Adnexal; Differential diagnosis; Case series; Retrospective study

* Corresponding author: AMAL AKAMMAR

Copyright © 2026 Author(s) retain the copyright of this article. This article is published under the terms of the Creative Commons Attribution License 4.0.

1. Introduction

The female pelvis encompasses a wide variety of anatomical structures whose pathological transformations may produce masses clinically and radiologically indistinguishable from ovarian neoplasms. Adnexal masses carry an incidence of 0.17% to 5.9% in asymptomatic women and 7.1% to 12% in symptomatic women, yet fewer than 25% are ultimately diagnosed as malignant [1]. Critically, approximately 5.1% of pelvic masses presumed to be of ovarian origin prove to be extra-ovarian in etiology [2]. This diagnostic pitfall may lead to unnecessary oophorectomy, delay in appropriate treatment of the underlying condition, and avoidable surgical morbidity.

Ultrasound (US) remains the recommended first-line imaging modality for any adnexal mass; however, its limitations frequently necessitate further evaluation. Computed tomography (CT) provides rapid anatomical assessment of the entire abdominopelvic cavity and is invaluable in emergency settings. Magnetic resonance imaging (MRI), with its superior soft-tissue contrast, multiplanar capability, and functional sequences (diffusion-weighted imaging [DWI], dynamic gadolinium enhancement), serves as the definitive problem-solving modality in most complex or indeterminate cases [3,4].

This retrospective series presents 241 cases of pelvic masses originally identified on US and further characterized on CT and/or MRI, collected over three years at CHU Hassan II, Fez, Morocco. All cases were classified as extra-ovarian based on histopathological findings, surgical records, or definitive multimodality imaging diagnosis. The objective of this article is to present the full spectrum of extra-ovarian etiologies encountered, describe their characteristic imaging features across modalities, highlight key differentiating signs, and illustrate selected cases with representative imaging descriptions. This work is intended as a practical educational resource for radiologists, gynecologists, and clinicians managing female patients with pelvic masses.

2. Materials and methods

2.1. Study Design and Patient Population

This is a single-center retrospective study conducted at the Radiology Department of the Mother and Child Hospital and the Hospital of Specialties, CHU Hassan II, Sidi Mohammed Ben Abdallah University, Fez, Morocco. All female patients presenting with a pelvic mass identified on initial ultrasound between January 2023 and December 2025 were eligible for inclusion. A total of 241 patients were enrolled.

2.2. Imaging Protocol

All patients underwent pelvic ultrasound (US) as the primary evaluation. Patients with inconclusive US findings, complex masses, or suspected malignancy subsequently underwent contrast-enhanced CT of the abdomen and pelvis and/or dedicated pelvic MRI. MRI protocols included T1-weighted, T2-weighted, fat-saturated T1, diffusion-weighted (DWI, b=0 and b=1000 s/mm^2), and dynamic gadolinium-enhanced sequences in axial, sagittal, and coronal planes.

2.3. Diagnostic Classification

Final diagnosis was established by histopathological analysis (surgical specimens or biopsy) in the majority of cases, supplemented by definitive radiological diagnosis in selected cases (e.g., hematoma, lymphocele, peritoneal inclusion cyst) where imaging findings were unequivocal and surgical confirmation was not performed. Cases were classified into six major categories based on anatomical origin: extra-ovarian adnexal lesions, uterine lesions, peritoneal disease, gastrointestinal lesions, extraperitoneal lesions, and collections. A total of twenty distinct etiologies were identified.

2.4. Ethical Considerations

This study was approved by the institutional review board of CHU Hassan II. Patient data were fully anonymized. Informed consent was waived given the retrospective design.

3. Results

3.1. Study Population

A total of 241 patients with a pelvic mass were included. The age range spanned from 17 to 86 years. All 241 masses were ultimately classified as extra-ovarian in origin. Twenty distinct etiologies were identified across six anatomical

categories. Table 1 presents the complete distribution of diagnoses with their respective case counts, key imaging features, and principal distinguishing clues.

Table 1 Distribution of Extra-Ovarian Pelvic Mass Etiologies and Key Imaging Features (N=241)

Category	Etiology	N	Key Imaging Features	Distinguishing Clue
A. EXTRA-OVARIAN ADNEXAL LESIONS				
Tubal	Hydrosalpinx / Hematosalpinx	13	C/S-shaped fluid-filled tubular structure; cogwheel sign on cross-section; T1 hyperintense content in hematosalpinx; mildly enhancing thin walls	Tubular morphology; normal ipsilateral ovary identified separately
Tubal	Pyosalpinx / Tubo-ovarian abscess	23	Thick-walled tubular structure; complex fluid ± debris; DWI restriction; perilesional fat stranding; internal gas in abscess; peripheral wall enhancement	Fever + elevated CRP; internal gas pathognomonic of TOA
Tubal	Adnexal ectopic pregnancy	13	Complex tubal mass separate from ovary; ring-of-fire on Doppler; ring-like gadolinium enhancement; T2 hyperintense sac with thick wall; ± hemoperitoneum	Elevated beta-hCG; reproductive age; tubal location
Torsion	Adnexal torsion	27	Enlarged, medially displaced ovary; whirlpool/twisted pedicle sign on CT/MRI; peripheralized follicles; absent or reduced Doppler flow; ± hemoperitoneum	Acute severe pelvic pain; twisted vascular pedicle on CT/MRI
Peritoneal	Peritoneal inclusion cyst	14	Cystic multilocular mass conforming to adjacent structures; entrapped ipsilateral ovary ('spider web' pattern); thin enhancing septa; no solid component	History of prior surgery/PID; 'spider web' pattern; entrapped ovary
B. UTERINE LESIONS				
Vascular	Uterine vasculature / varices	9	Serpiginous perivascular structures; enhancement identical to iliac vessels on CT/MRI; thrombosis may be present; no true mass	Enhancement kinetics matching vessels; Doppler confirmation
Myometrial	Leiomyoma FIGO 7 (pedunculated)	17	T2 hypointense whorled mass; bridging vessel sign (stalk connecting to uterus); claw sign; heterogeneous enhancement; calcifications possible	Bridging vessel/stalk to uterus; T2 hypointensity; prior history of fibroids
C. PERITONEAL DISEASE				
Malignant	Peritoneal carcinomatosis	12	Small irregular peritoneal nodules; omental caking; proteinaceous ascites; DWI	Known primary malignancy; omental caking; multifocal peritoneal nodules

			restriction; mucinous deposits show low CT attenuation	
Infectious	Peritoneal tuberculosis	8	Ascites with peritoneal thickening/nodularity; central low-attenuation lymph nodes; soft tissue masses; no dominant adnexal mass	Endemic country; systemic symptoms; peritoneal biopsy confirmation
D. GASTROINTESTINAL LESIONS				
Inflammatory	Appendicitis / Diverticulitis	21	Non-compressible appendix >6 mm ± periappendiceal fat stranding; sigmoid wall thickening with pericolic fat stranding in diverticulitis; phlegmon/abscess	Right/left iliac fossa pain; adjacent bowel involvement
Tumoral	Appendiceal mucocele	10	Tubular cystic appendiceal dilation; 'onion skin' sign (US); simple fluid ± calcifications; wall enhancement if superinfected; ± peritoneal mucin if ruptured	'Onion skin' sign; cecal tip origin; risk of pseudomyxoma peritonei
Tumoral	GIST	5	Large intraperitoneal mass; intermediate T2 signal; internal necrosis (T2 hyperintense areas); DWI restriction; heterogeneous enhancement; large peritoneal effusion	Both ovaries identified separately; organ of origin traceable
Tumoral	Sigmoid tumor process	7	Asymmetric sigmoid wall thickening; irregular luminal narrowing; pericolic fat infiltration; lymphadenopathy; associated with rectal bleeding	Rectal bleeding; annular morphology; colonoscopic confirmation
E. EXTRAPERITONEAL LESIONS				
Lymphatic	Necrotic lymphadenopathy	11	Enlarged pelvic lymph nodes; central necrosis and heterogeneous enhancement; bilateral lumbosacral distribution; ± associated primary tumor	Extraperitoneal compartment; associated primary malignancy
Lymphatic	Lymphoma	7	Homogeneous mass encasing vessels without compression; mild-to-moderate enhancement; iso-T1/iso-T2; multi-station adenopathy; splenomegaly	Systemic B symptoms; multi-station disease; encasement without compression
Mesenchymal	Sarcoma	3	Soft tissue mass centered on bony/muscular pelvic structures; isointense T1 with heterogeneous enhancement; both ovaries normal	Young patient; obturator/pelvic wall origin; both ovaries normal
Neurogenic	Neurogenic tumors (schwannoma, neurofibroma,	4	Extraperitoneal paravertebral/parametrial mass; low T1/high T2	Paravertebral location; target sign; elevated catecholamines

	ganglioneuroma, paraganglioma)		(schwannoma); target sign on T2 (neurofibroma); avid enhancement ± catecholamines (paraganglioma)	
Neurogenic	Pelvic pheochromocytoma	1	Heterogeneous T2 hyperintense parametrial mass; early avid enhancement; necrotic areas; normal ovaries; elevated plasma catecholamines	Hypertension + elevated catecholamines; risk of crisis if biopsied without alpha-blockade
F. COLLECTIONS (INTRA- OR EXTRAPERITONEAL)				
Traumatic/Post-op	Hematoma	23	Hyperattenuating on CT (acute); evolving signal on MRI (T1 high on fat-sat, concentric ring sign in chronic); no postcontrast enhancement; ± active bleeding	History of surgery/trauma/coagulopathy; evolving imaging appearance
Post-surgical	Lymphocele / Seroma	13	Simple non-enhancing fluid collection along lymphatic chain; T1 hypo / T2 hyper; thin enhancing wall; mass effect on adjacent structures; develops 3–8 weeks post-op	History of lymphadenectomy; simple fluid; no enhancement; delayed onset post-op

3.2. Category Distribution

The most frequently encountered etiology was adnexal torsion (n=27, 11.2%), followed by hematoma (n=23, 9.5%), pyosalpinx/tubo-ovarian abscess (n=23, 9.5%), pedunculated leiomyoma FIGO 7 (n=17, 7.1%), peritoneal carcinomatosis (n=12, 5.0%), and necrotic lymphadenopathy (n=11, 4.6%). The complete distribution of all twenty etiologies with their respective case counts is presented in Table 1. Rare etiologies included pelvic pheochromocytoma (n=1, 0.4%) and sarcoma (n=3, 1.2%), which nonetheless presented diagnostic challenges due to their potentially aggressive nature.

3.3. Imaging Modality Performance

Ultrasound served as the primary screening tool in all 241 cases. CT was performed in 189 cases (78.4%), primarily for characterization of large masses, acute presentations, and suspected gastrointestinal or extraperitoneal lesions. MRI was performed in 203 cases (84.2%) and proved decisive in resolving diagnostic ambiguity in 168 of these (82.8%). DWI sequences were particularly valuable in differentiating pyogenic collections (high b1000 signal, low ADC), lymphoma (intermediate diffusion), and peritoneal carcinomatosis from benign conditions. Gadolinium-enhanced sequences were essential for characterizing wall enhancement in tubal pathology, peritoneal disease, and neurogenic tumors.

3.4. Illustrated Case Reports

The following ten cases were selected from the series to illustrate the key imaging features of the most instructive and representative etiologies. Each case highlights practical differentiating signs applicable in daily radiological practice.

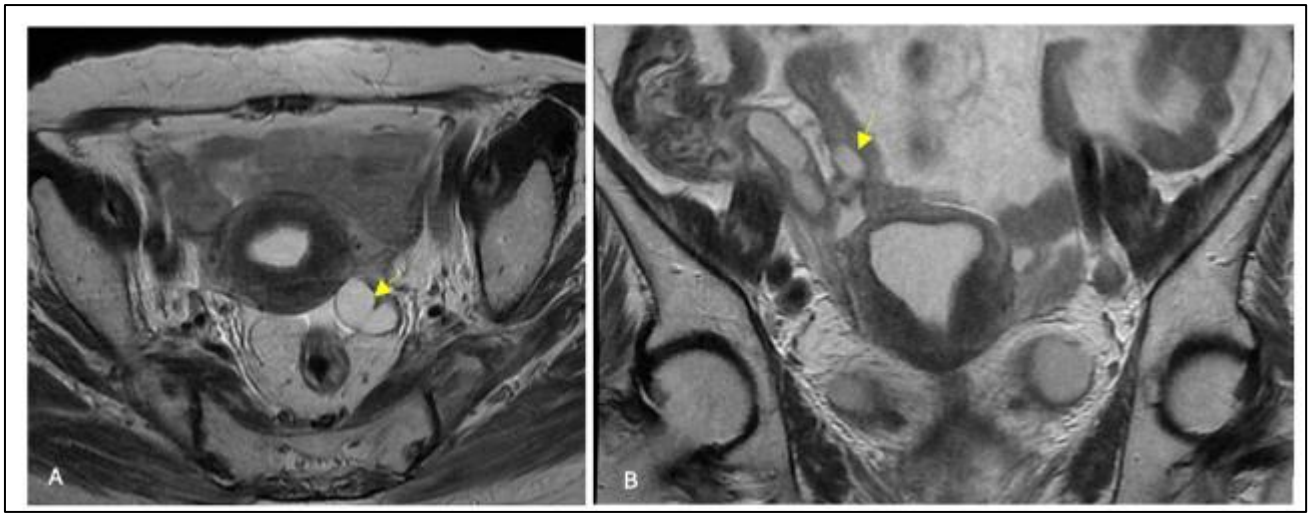

Demographics: Female, 74 years old. Postmenopausal; **Presentation**: Known cervical cancer, previously treated with external radiotherapy and brachytherapy. Incidental finding on follow-up MRI; **Imaging Findings**: Axial (A) and coronal (B) T2-weighted MRI: Bilateral dilated, tortuous fallopian tubes with simple fluid content. The left tube is more prominently enlarged. Tubular morphology preserved with a 'cogwheel' internal architecture on cross-sectional views. Thin mildly enhancing walls. No internal complexity or solid components. Both ovaries identified separately; **Diagnosis**: Bilateral hydrosalpinx secondary to post-radiation adhesive disease; **Key Imaging Pearl**: The C/S-shaped tubular morphology with a 'cogwheel' appearance on cross-sectional views is pathognomonic of hydrosalpinx. Identification of the normal ovary adjacent to but clearly separate from the tubular structure is essential to exclude ovarian origin.

Figure 1 Hydrosalpinx — Bilateral Post-Radiation Tubal Dilation

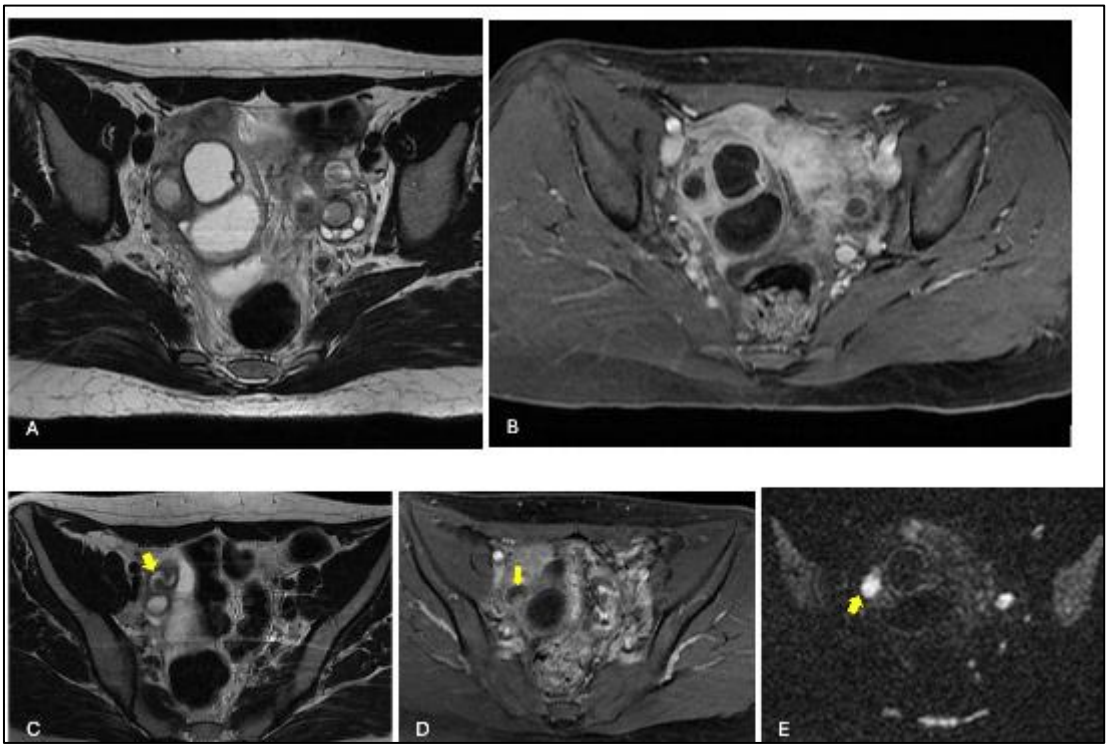

Demographics: Female, 27 years old. No prior medical history; **Presentation**: Pelvic pain persisting for 5 months. Elevated inflammatory markers (WBC, CRP); **Imaging Findings**: MRI multisequence: Axial images in different sequences shows a right lateral uterine rounded formation, well-defined with regular contours, described as hypo-intense on T1, hyper-intense on T2 (A), with a hypo-intense T2 wall and enhancement after contrast injection (B). Associated with the presence of a tubal structure adjacent to the uterus (yellow arrow), with hypo-intense T1 content (D), hyper-intense T2 content (C), partially restrictive on diffusion (E), and a thickened wall that enhances after contrast injection (D); **Diagnosis**: Right ovarian abscess with concurrent right pyosalpinx in the setting of pelvic inflammatory disease. Managed conservatively with broad-spectrum antibiotics; **Key Imaging Pearl**: The co-existence of a complex adnexal mass with wall thickening, DWI restriction, and an adjacent thickened tubular structure is highly characteristic of TOA with pyosalpinx. Perilesional fat stranding and clinical context (fever, elevated CRP) complete the diagnosis. Surrounding inflammatory change differentiates pyosalpinx from hydrosalpinx.

Figure 2 Tubo-Ovarian Abscess with Concurrent Pyosalpinx

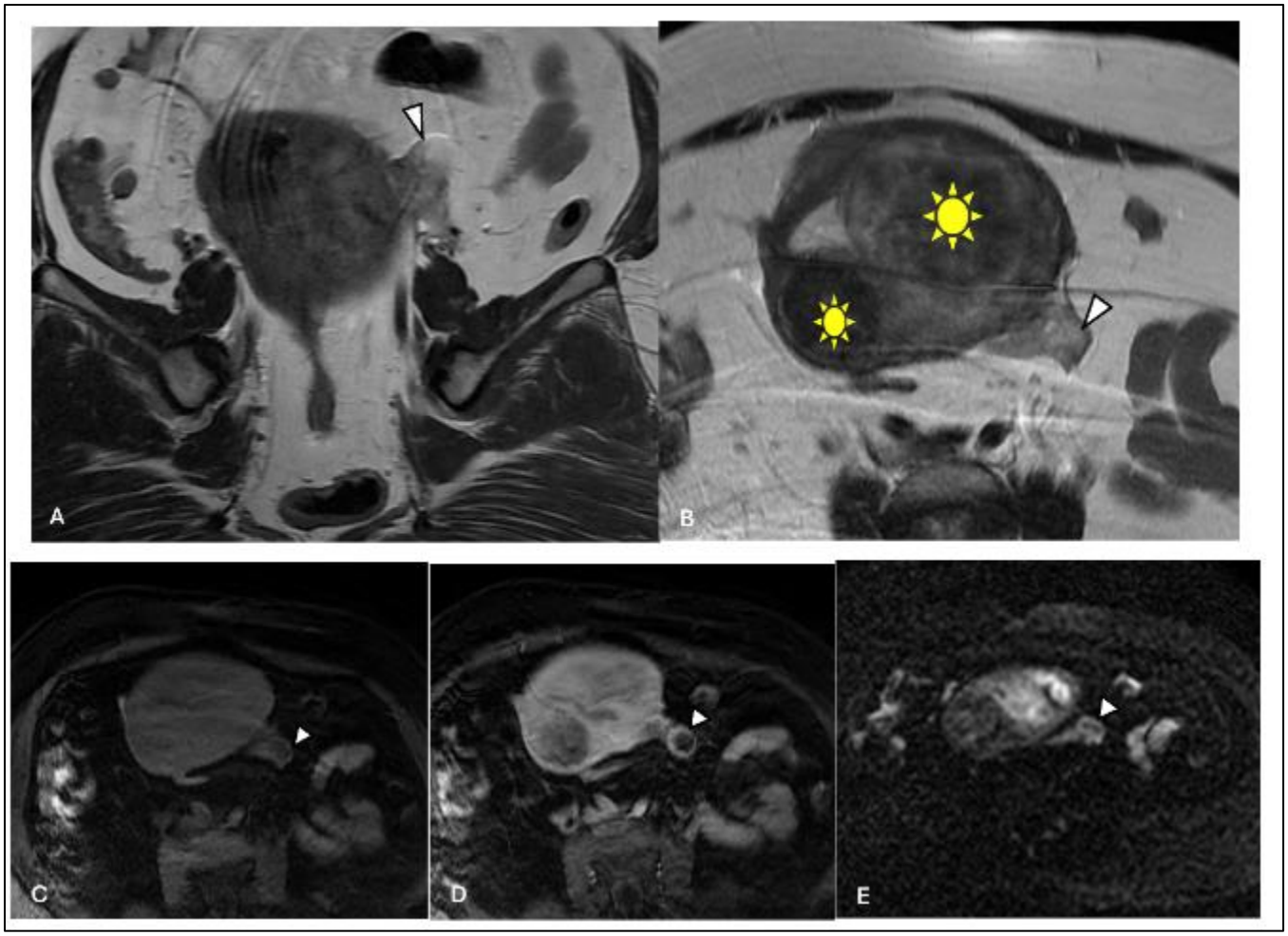

Demographics: Female, 40 years old. G6P5.

Presentation: 10 weeks of amenorrhea, markedly elevated beta-hCG. No acute abdomen on presentation.

Imaging Findings: Pelvic MRI: The left fallopian tube is swollen with a cystic intraluminal formation affecting its ampullary portion (headarrow), described as hyperintense on axial (B) and coronal (A) T2-weighted images, and hypointense on T1-weighted image (C), surrounded by a thick wall with hyperintensity on diffusion (E) and early ring-like enhancement after GADO injection (D), measuring 25 x 20 mm, consistent with an adnexal ectopic pregnancy. Note the presence of a polymyomatous uterus ( ) .

Diagnosis: Left ampullary ectopic pregnancy. Managed by left salpingectomy.

Key Imaging Pearl: Ectopic pregnancy must be considered whenever a complex adnexal tubular mass is identified in a woman of reproductive age with elevated beta-hCG. Ring-like gadolinium enhancement around a T2 hyperintense intraluminal structure in the fallopian tube, separate from the normal ovary, is characteristic. Absence of an intrauterine gestational sac on MRI is confirmatory.

Figure 3 Left Ampullary Ectopic Pregnancy

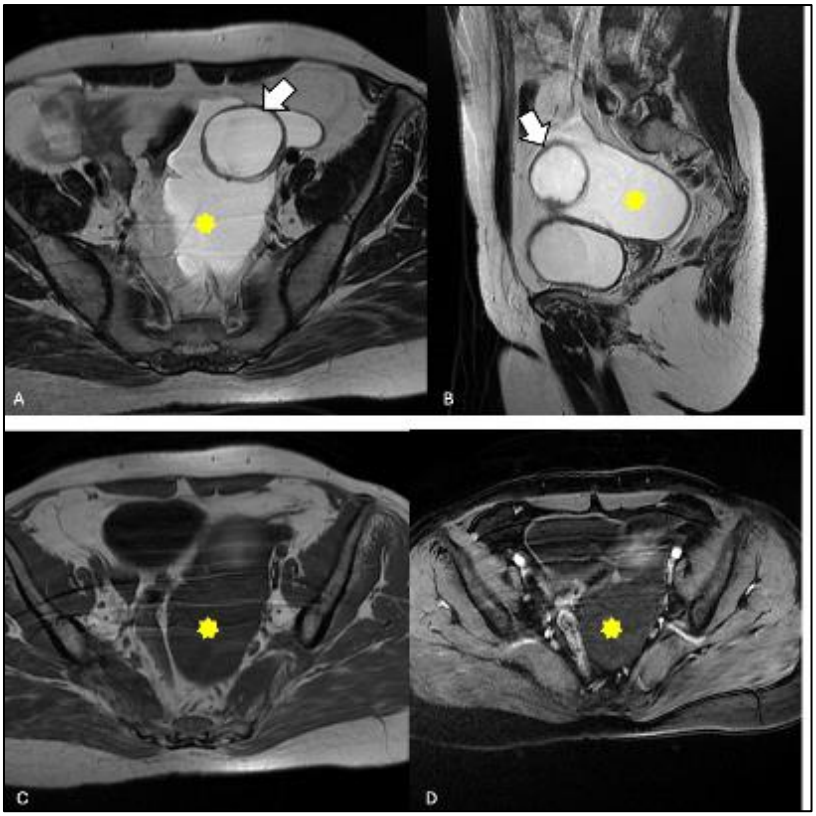

Demographics: Female, 42 years old. Perimenopausal. Underwent surgery in January 2022 for inter-adnexal hysterectomy (histopathology: leiomyoma); **Presentation**: Right pelvic pain. Prior inter-adnexal hysterectomy (January 2022) for uterine leiomyoma; **Imaging Findings**: MRI: shows a left ovarian lesion (white arrow), rounded and well-defined, hyperintense on both T1 (C) and T2 sequences (A,B) not suppressed on FAT-SAT, unchanged after contrast, with a thin wall enhanced after Gadolinium injection (D); Left-sided pelvic cystic formation ( ), hypointense on T1, hyperintense on T2, containing fine septa enhanced after contrast, without tissue bud within, consistent with peritoneal inclusion cyst; **Diagnosis**: Left endometrioma with concurrent left peritoneal inclusion cyst; **Key Imaging Pearl**: Peritoneal inclusion cysts conform to adjacent structures and characteristically envelop a normal, identifiable ovary in a 'spider web' pattern. Prior pelvic surgery or inflammatory condition is the key clinical trigger. Fine enhancing septa without solid components and absence of malignant features distinguish this entity from cystic ovarian neoplasms.

Figure 4 Peritoneal Inclusion Cyst (Post-Hysterectomy)

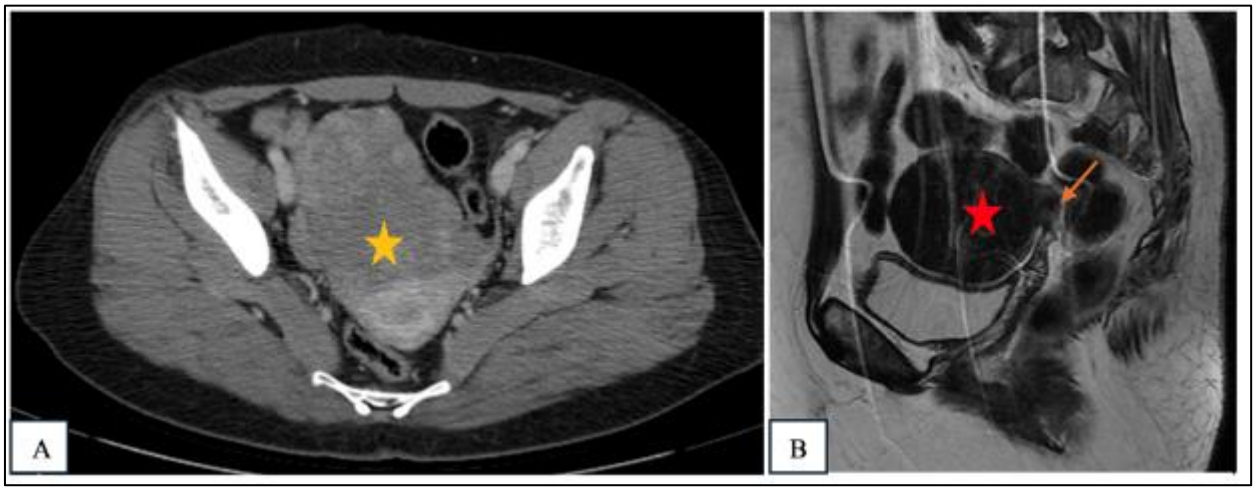

Demographics: Female, 47 years old. No significant medical history; **Presentation**: Pelvic pain. Pelvic ultrasound: solid right lateral uterine mass; **Imaging Findings**: CT (contrast-enhanced, axial): Heterogeneously enhancing pelvic mass in contact with the ovaries, uterus, small bowel loops, and bladder; **MRI (sagittal T2**): T2 hypointense mass with whorled internal architecture, pedunculated from the right anterolateral uterine surface near the uterine horn junction, with a connecting stalk of 12.5 mm, demonstrating the bridging vessel sign. Claw sign also present; Diagnosis: Pedunculated subserosal uterine leiomyoma (FIGO type 7). Managed with myomectomy; **Key Imaging Pearl**: The bridging vessel sign, a vascular pedicle directly connecting the mass to the uterus on Doppler US or MRI is the most reliable indicator of uterine origin for a solid pelvic mass. T2 hypointensity with a whorled architecture distinguishes leiomyoma from ovarian neoplasms. Without these signs, a pedunculated leiomyoma may be indistinguishable from a solid ovarian mass.

Figure 5 Pedunculated Subserosal Uterine Leiomyoma (FIGO 7)

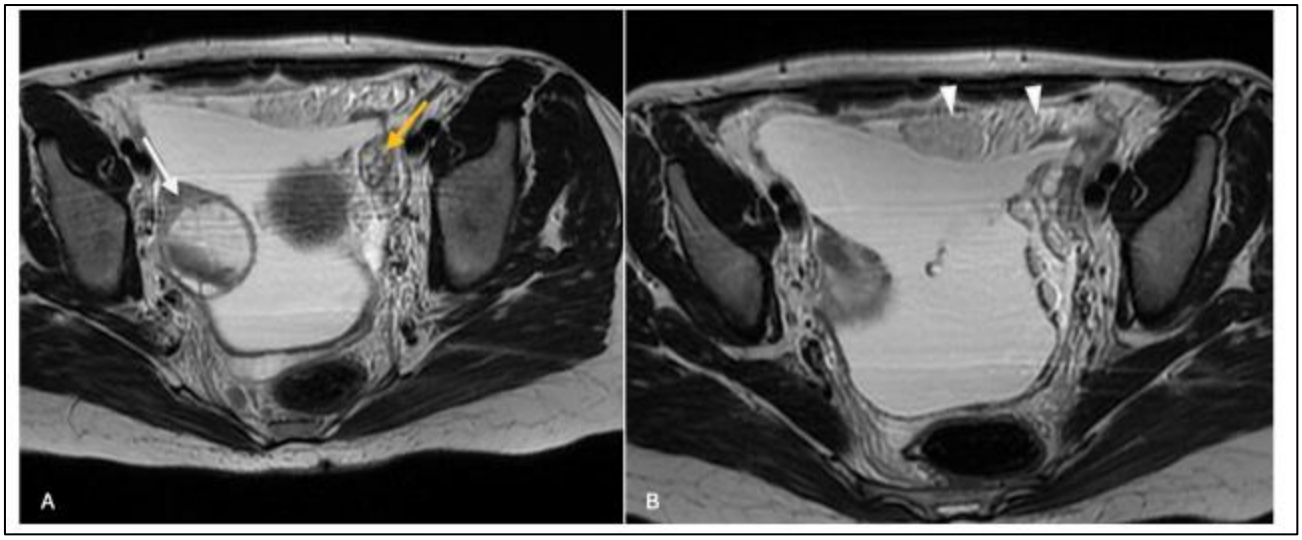

Demographics: Female, 22 years old.

Presentation: Pelvic pain, fever, weight loss, and asthenia (deteriorated general condition). Peritoneal biopsy confirmed the diagnosis.

Imaging Findings: Pelvic MRI (T2 axial): Right ovarian cystic lesion with hemorrhagic sediment content; left ovary multifollicular. Moderate ascites with regular thickening and nodularity of the peritoneal lining. No dominant solid adnexal mass. CT (when available) further demonstrates soft tissue peritoneal nodules with central low attenuation and enlarged lymph nodes with necrotic centers.

Diagnosis: Peritoneal tuberculosis with secondary reactive adnexal changes. Treated with standard four-drug anti-tuberculous chemotherapy.

Key Imaging Pearl: Peritoneal tuberculosis accounts for approximately 37.2% of pelvic masses mimicking ovarian tumors in endemic regions [2]. The clinical triad of ascites, regular peritoneal thickening/nodularity, and centrally necrotic lymphadenopathy in a young patient from an endemic country should prompt this diagnosis before attributing findings to peritoneal carcinomatosis.

Figure 6 Peritoneal Tuberculosis

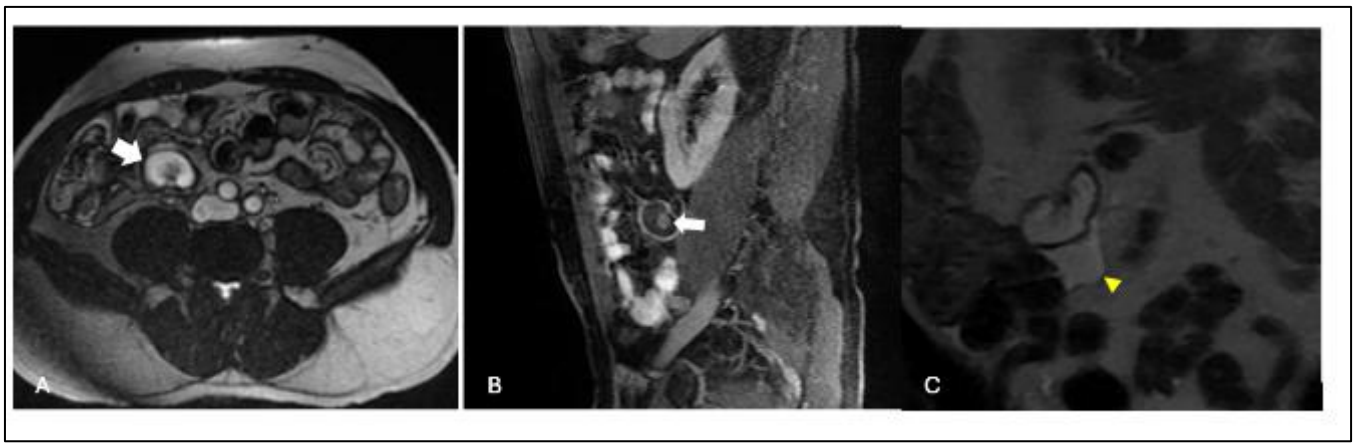

Demographics: Female, 62 years old; **Presentation**: Chronic right iliac fossa pain; **Imaging Findings**: MRI (multisequence): (A ET B) Cystic dilation of the appendix with fluid content T1 hypointense with wall enhancement on sagittal T1 gadolinium , T2 hyperintense on axial FIESTA. 'Onion skin' sign identifiable on cross-sectional views. Intraperitoneal fluid effusion in contact with the appendix suggesting rupture. No pseudomyxoma peritonei pattern at the time of imaging; **Diagnosis**: Appendiceal mucocele (low-grade mucinous neoplasm) with rupture. Surgical resection performed. No pseudomyxoma peritonei at surgery; **Key Imaging Pearl**: The 'onion skin' sign on US/MRI concentric rings within the appendiceal lumen is the specific marker of appendiceal mucocele. A right adnexal cystic mass should always prompt careful examination of the cecal tip region. Rupture may result in pseudomyxoma peritonei, a life-altering complication requiring radical debulking surgery and intraperitoneal chemotherapy.

Figure 7 Appendiceal Mucocele with Rupture

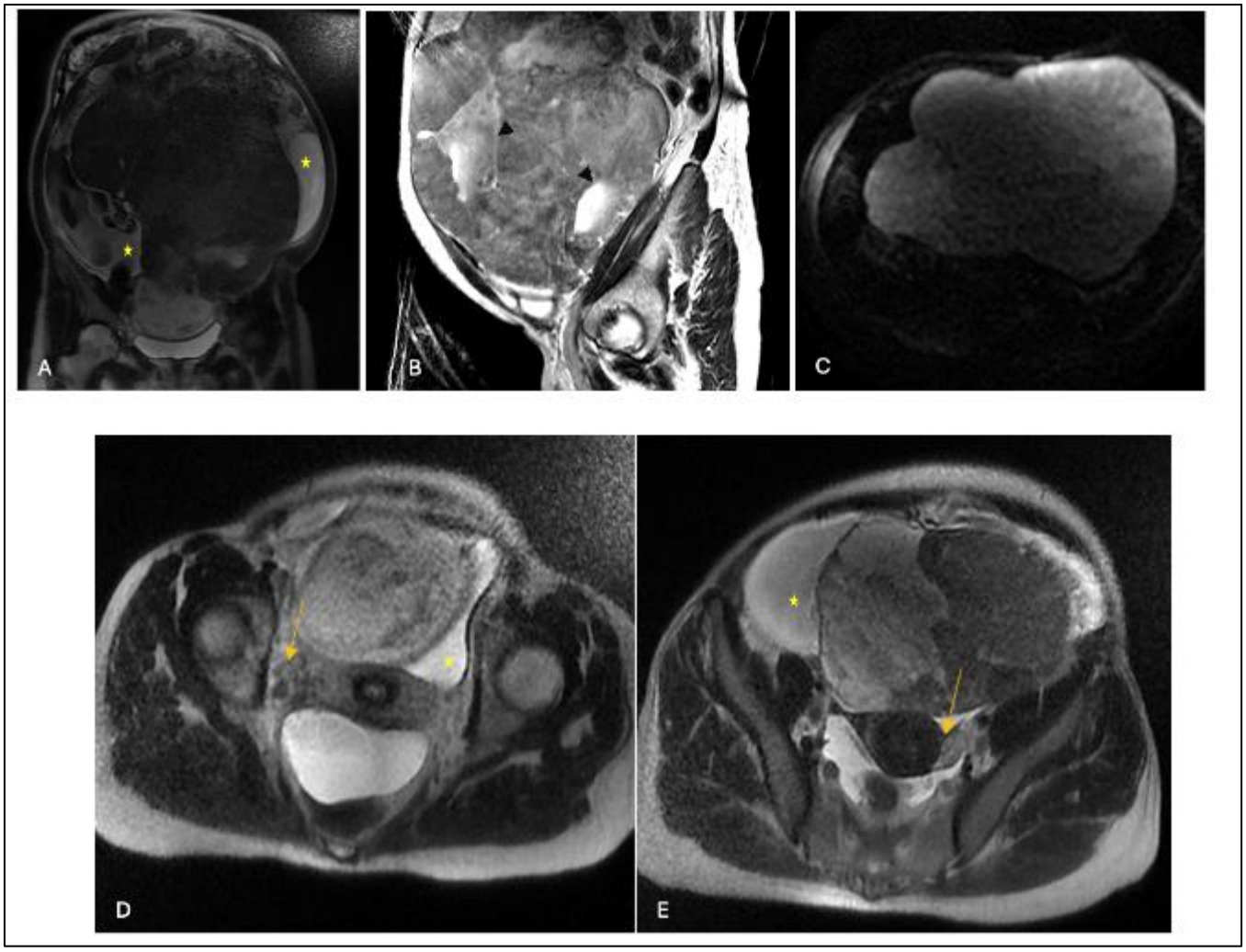

Demographics: Female, 45 years old. No significant medical history; Presentation: Hard, non-mobile hypogastric mass. Biopsy: GIST.

Imaging Findings: MRI : shows a large intra-peritoneal mass, well-defined but with irregular contours, described as having an intermediate signal on T2 (A,B), containing T2 hyperintense corresponding to areas of necrosis (headarrows), with diffusion restriction (C). It features also multiple fine septa; Ovaries are small in size and appear normal in axial T2 (D, E) (orange arrows); Large intra-peritoneal effusion, described as hyperintense fluid on T2 (yellow star).

Diagnosis: Gastrointestinal stromal tumor (GIST) of probable small bowel origin. Treated with surgical resection and imatinib.

Key Imaging Pearl: Identification of both normal ovaries separately from a large intraperitoneal mass is the decisive step in excluding ovarian origin. GISTs characteristically show intermediate T2 signal with internal necrosis and heterogeneous enhancement. Tracing the feeding mesenteric vessel or mass-bowel interface identifies the organ of origin. Biopsy confirmation and KIT immunohistochemistry are required for definitive diagnosis.

Figure 8 Gastrointestinal Stromal Tumor (GIST)

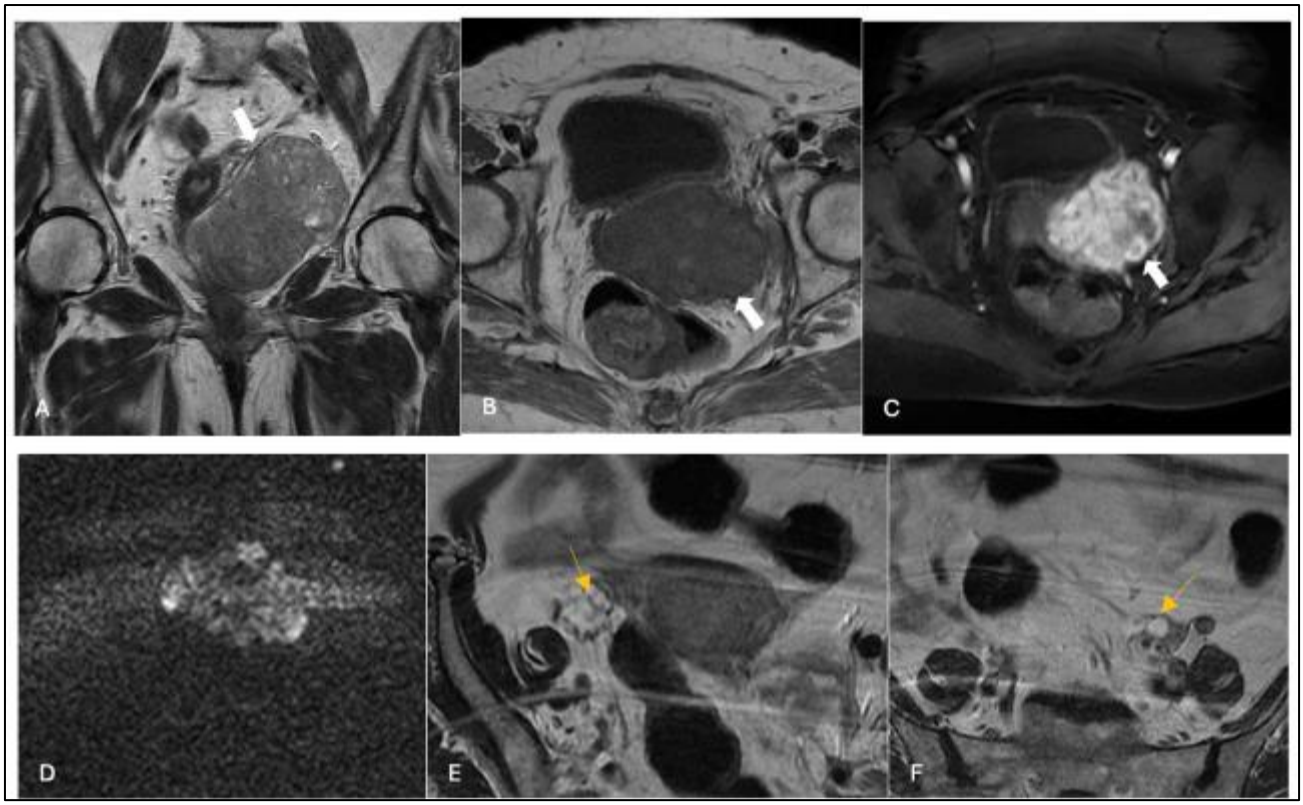

Demographics: Female, 86 years old; **Presentation**: Lateral uterine mass detected incidentally. Subsequent workup revealed markedly elevated plasma and urinary catecholamine levels; **Imaging Findings**: MRI : MRI findings demonstrating a large left parametrial pelvic mass (white arrows), described as heterogeneous T2 hyperintense (A), containing necrotic areas in T1 hypointense with hemorrhagic changes (B), a hyperintense in diffusion sequence (D), and showing an early and intense enhancement after contrast (C). the both ovaries are seen (orange arrows), without any anomaly (E, F); **Diagnosis**: Extra-adrenal pheochromocytoma (paraganglioma) of the left parametrium. Managed with surgical resection after preoperative alpha-adrenergic blockade. Key Imaging Pearl: An y avidly enhancing parametrial or retroperitoneal pelvic mass in a patient with hypertension or elevated catecholamines should raise suspicion for paraganglioma. Biopsy without prior alpha-blockade carries a life-threatening risk of hypertensive crisis. Functional imaging (MIBG scintigraphy or DOTATATE PET-CT) is essential before surgical planning.

Figure 9 Extra-Adrenal Pheochromocytoma (Pelvic Paraganglioma)

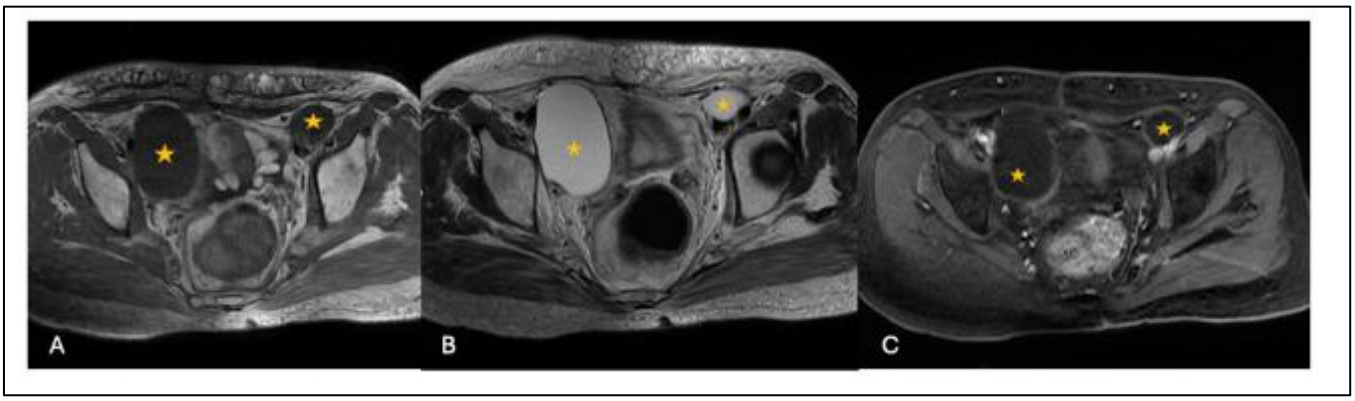

Demographics: Female, 56 years old; **Presentation**: Follow-up MRI for endometrial adenocarcinoma, post-total hysterectomy, bilateral adnexectomy, pelvic and lombo-aortic lymphadenectomy, external radiotherapy, and brachytherapy; **Imaging Finding**s: Pelvic MRI (multisequence): MRI findings demonstrate two bilateral external iliac pelvic cystic formations (yellow star), described as T1 hypointense (A), T2 hyperintense (B), with thin walls enhanced after contrast (C), exhibit a slightly mass effect on the adjacent pelvic structures, consisting with seromas. Uterus and ovaries absent (consistent with prior surgery); **Diagnosis**: Bilateral post-lymphadenectomy seromas/lymphoceles. Managed conservatively with imaging follow-up; **Key Imaging Pearl**: Post-operative lymphoceles and seromas are simple non-enhancing fluid collections that typically develop 3–8 weeks after pelvic lymphadenectomy. Their location along the iliac lymphatic chain, simple T1/T2 signal, thin enhancing wall, and absence of solid elements or DWI restriction reliably distinguish them from recurrent malignancy or cystic ovarian lesions. Surgical history is the single most important contextual clue.

Figure 10 Post-Lymphadenectomy Seroma / Lymphocele

4. Discussion

This retrospective series of 241 patients presenting with pelvic masses ultimately classified as extra-ovarian demonstrates the breadth and clinical significance of pathologies that may masquerade as ovarian neoplasms. Indeed, up to 5.1% of pelvic masses presumed to be ovarian are ultimately of extra-ovarian origin, underscoring the need for a rigorous multimodality imaging approach [1,2]. The following discussion addresses the key diagnostic strategies and specific findings observed across our cohort.

The fundamental first step in any pelvic mass evaluation is the identification of both normal ovaries separately from the mass. The ovarian vascular pedicle sign and phantom organ sign were the two most decisive tools applied across our series When the ipsilateral ovary could not be identified—suggesting ovarian origin—surgical pathology was sought. When both ovaries were clearly separate from the mass, extra-ovarian etiologies were systematically pursued [5,6,7].

Anatomical compartment analysis was the second decisive layer of assessment. Correct assignment of a mass to the extraperitoneal compartment categorically excluded ovarian origin and directed the differential toward retroperitoneal, parametrial, and post-surgical pathologies [8,9]. Intraperitoneal masses required a broader differential spanning adnexal, uterine, peritoneal, and gastrointestinal etiologies.

MRI emerged as the definitive problem-solving modality across all categories, proving decisive in 82.8% of cases where it was performed. DWI sequences were particularly valuable for the characterization of pyogenic collections, lymphoma, and peritoneal carcinomatosis. Gadolinium-enhanced sequences were essential in all cases involving wall assessment, vascularity, or enhancement kinetics. These findings align with the established literature on MRI superiority for female pelvic mass characterization [3,4].

The most frequent etiology in our series was adnexal torsion (n=27, 11.2%), an emergency condition that, when it involves the fallopian tube exclusively (as in five of our cases) can be particularly challenging to diagnose, since the ovary may appear normal. The presence of a twisted vascular pedicle on CT or MRI, even in the absence of ovarian enlargement, is sufficient to prompt surgical exploration [10,11,12]. Hematoma (n=23, 9.5%) and tubo-ovarian abscess with pyosalpinx (n=23, 9.5%) were equally common, both presenting in acute or subacute settings and requiring urgent clinical management.

Peritoneal tuberculosis (n=8) deserves particular emphasis given its high prevalence in our North African context. As reported in the literature, it accounts for up to 37.2% of pelvic masses mimicking ovarian tumors in endemic regions [2]. The combination of ascites, peritoneal nodularity, and centrally necrotic lymphadenopathy in a young patient with deteriorated general condition should prompt this diagnosis before attributing findings to carcinomatosis.

Rare but high-stakes diagnoses included pelvic pheochromocytoma (n=1) and sarcomas (n=3). The pheochromocytoma case illustrates a critical safety point: any avidly enhancing pelvic mass in a patient with catecholamine excess must be recognized before biopsy is attempted, as unblocked catecholamine release during tissue sampling can cause life-threatening hypertensive crisis. Functional imaging with MIBG scintigraphy or DOTATATE PET-CT should precede any invasive procedure [13].

5. Conclusion

This series of 241 patients with extra-ovarian pelvic masses demonstrates that a systematic multimodality imaging approach combining anatomical compartment analysis, specific imaging signs, functional MRI sequences, and clinical correlation is essential for accurate pre-operative diagnosis. The twenty etiologies identified span a broad spectrum from benign and self-limiting conditions to surgical emergencies and rare malignancies. Recognizing the characteristic imaging fingerprint of each entity prevents unnecessary oophorectomy, guides appropriate management, and optimizes patient outcomes. MRI, with its superior soft-tissue contrast and functional capabilities, remains the cornerstone problem-solving modality in this context.

Compliance with ethical standards

Disclosure of conflict of interest

No conflict of interest to be disclosed.

Statement of ethical approval

This retrospective study was approved by the Institutional Review Board of our University Hospital.

Statement of informed consent

Informed consent was obtained from all individual participants included in the study."

References

[1] Rajkotia K, Veeramani M, Macura KJ. Magnetic resonance imaging of adnexal masses. Top Magn Reson Imaging. 2006;17:379–397.

[2] Ozat M, Altinkaya SO, Gungor T, et al. Extraovarian conditions mimicking ovarian cancer: A single center experience of 15 years. Arch Gynecol Obstet. 2011;284:713–719.

[3] Nougaret S, Nikolovski I, Paroder V, et al. MRI of Tumors and Tumor Mimics in the Female Pelvis: Anatomic Pelvic Space-based Approach. Radiographics. 2019;39:1205–1229.

[4] Shetty M. Nonovarian Mimics of Ovarian Malignancy. Semin Ultrasound CT MRI. 2019;40:319–331.

[5] Saksouk FA, Johnson SC. Recognition of the ovaries and ovarian origin of pelvic masses with CT. Radiographics. 2004;24(Suppl 1):S133–S146.

[6] Lee JH, Jeong YK, Park JK, Hwang JC. Ovarian vascular pedicle sign revealing organ of origin of a pelvic mass lesion on helical CT. Am J Roentgenol. 2003;181:131–137.

[7] Oliveira JD, Cunha TM, Tereso A. Tumors of the broad ligament. Radiol Bras. 2020;53:349–355.

[8] Levy AD, Shaw JC, Sobin LH. Secondary tumors and tumorlike lesions of the peritoneal cavity. Radiographics. 2009;29:347–373.

[9] O'Connell AM, Duddy L, Lee C, Lee MJ. CT of pelvic extraperitoneal spaces: An anatomical study in cadavers. Clin Radiol. 2007;62:432–438.

[10] Dawood MT, Naik M, Bharwani N, et al. Adnexal Torsion: Review of Radiologic Appearances. Radiographics. 2021;41:609–624.

[11] Singh A, Danrad R, Hahn PF, et al. MR imaging of the acute abdomen and pelvis. Radiographics. 2007;27:1419–1431.

[12] Rha SE, Byun JY, Jung SE, et al. CT and MR imaging features of adnexal torsion. Radiographics. 2002;22:283–294.

[13] Rha SE, Byun JY, Jung SE, et al. Neurogenic tumors in the abdomen: Tumor types and imaging characteristics. Radiographics. 2003;23:29–43.